Neuroscience Letters 487 (2011) 113–117

Contents lists available at ScienceDirect

Neuroscience Letters

journal homepage: www.elsevier.com/locate/neulet

Discrimination of AD and normal subjects from MRI: Anatomical versus statistical regions

Mariola Pelaez-Coca*, Matias Bossa, Salvador Olmos, The Alzheimer's Disease Neuroimaging Initiative (ADNI)[1]

GTC, Aragon Institute of Engineering Research, Universidad de Zaragoza, Building I+D, C/Mariano Esquillor S/N, 50018 Zaragoza, Spain

ARTICLE INFO

Article history:
Received 2 June 2010
Received in revised form 1 October 2010
Accepted 4 October 2010

Keywords:
Alzheimer's disease
Feature extraction
Student's *t*-test
Anatomical masks
Classification

ABSTRACT

This work is a feature-extraction and classification study between Alzheimer's disease (AD) patients and normal subjects. Voxel-wise morphological features of brain MRI are defined as the Jacobian determinants that measure the local volume change between each subject and a given atlas. The goal of this work is to determine the region of interest (ROI) which is best suited for classification. Two types of ROIs are considered: anatomical regions, that were automatically segmented in the atlas (amygdalae, hippocampi and lateral ventricles); and statistical regions, defined from group comparison statistical maps. Classification performance was assessed with five classifiers on 20 pairs of matched training and test groups of subjects from the ADNI database. In this study the statistical masks provided the best classification performance.

Alzheimer's disease (AD) is the most common neurodegenerative illness, accounting for 60–70% of age-related dementia cases [27]. In 2000, approximately 24 million people over the age of 60 were diagnosed with dementia worldwide, and this number is expected to reach over 81 million by 2040 [7].

The Alzheimer's Disease Neuroimaging Initiative (ADNI) [19] is a large multi-site longitudinal structural Magnetic Resonance Imaging (MRI) and Fluorodeoxyglucose Positron Emission Tomography (FDG-PET) study of 800 adults, ages 55–90, including 200 elderly controls, 400 subjects with Mild Cognitive Impairment (MCI), and 200 patients with AD. The ADNI was launched in 2003 by National Institute on Aging, National Institute of Biomedical Imaging and Bioengineering, Food and Drug Administration, private pharmaceutical companies and non-profit organizations, as a $60 million, 5-year public–private partnership. The primary goal of ADNI has been to test whether serial MRI, PET, other biological markers, and clinical and neuropsychological assessment can be combined to measure the progression of MCI and early AD.

MRI is widely used in AD studies as it can non-invasively quantify gray and white matter integrity with high reproducibility [17]. MRI-based measures of cortical and hippocampal atrophy have been used in clinical trials [11,15], and they have been shown to correlate with pathologically confirmed neuronal loss and with the molecular hallmarks of AD [14,22]. In recent years, multivariate pattern recognition methods have been proposed to classify AD versus normal subjects [4,9,26]. In order to reduce data dimensionality a mask is usually defined, either by thresholding a Student's *t*-test map [9,26], or by selecting a ROI from automatic segmentation of anatomical structures [9]. Voxel-based features from a large rectangular region of interest (ROI) in the medial temporal lobe were used in [4].

Several type of MRI features have been used for AD classification, such as image intensity [4], tissue density [26], Jacobian determinant [4], boundary shape descriptors based on SPHARM-PDM (Spherical Harmonics-Point Distribution Model) [9]. On the other hand, gender and age may be relevant information for AD discriminate [16], being old age the largest risk factor [5]. In addition, the ApolipoproteinE (ApoE) genotype is linked to AD risk, where the presence of $\epsilon 4$ allele increases the AD risk while $\epsilon 2$ is protective [1]. Vemuri et al. [26] included these demographic variables to improve classification accuracy.

In this study, three major design criteria for the classification algorithm were used: generalizability, small number of features, and amenability to anatomical interpretation of the selected features. To ensure the generalization of the results, an evaluation that included 20 random allocation of pairs of training and testing groups was carried out. This type of evaluation has not been taken

* Corresponding author. Dep. Ingeniería Electrónica y Comunicaciones, Edificio Ada Byron, Universidad de Zaragoza, María de Luna n°1, 50018 Zaragoza, Spain. Tel.: +34 976762875; fax: +34 976 762111.
E-mail address: mdpelaez@unizar.es (M. Pelaez-Coca).

[1] Data used in the preparation of this article were obtained from the Alzheimer's Disease Neuroimaging Initiative (ADNI) database (www.loni.ucla.edu/ADNI). As such, the investigators within the ADNI contributed to the design and implementation of ADNI and/or provided data but did not participate in analysis or writing of this report. For a complete list of investigators involved in ADNI see: http://www.loni.ucla.edu/ADNI/About/About_InvestigatorsTable.shtml.

0304-3940/$ – see front matter © 2010 Elsevier Ireland Ltd. All rights reserved.
doi:10.1016/j.neulet.2010.10.007

into account in other papers [4,9,26]. A small number of features results in simpler and more robust classifiers. Thirdly, providing an anatomical interpretation of the selected features may help to understand the disease. It is well known that AD has a pattern of atrophy starting in the temporal lobe, mainly at entorhinal cortex and hipocampi, distributing throughout the cortex [21,25,3]. This atrophy is accompanied by lateral ventricle expansion [6,25].

The goal of this work was to determine which ROI is better suited for classification of normal versus AD subjects. Two types of ROIs were explored: anatomically defined masks and statistical masks. Amygdalae, hippocampi, and lateral ventricles were selected as anatomical masks for their relationship with AD [21,6,25,3]. The statistical masks were defined by thresholding a Student's *t*-test map in the whole brain, identifying the voxels with the most significant differences in volume between the two patient groups. In this paper we studied whether these voxels are adequate for classifying subjects. The study was focused on the determination of the masks rather than in the classifier design, therefore five standard classifiers were used. As in neuroimaging studies the number of voxels in each mask is much larger than the number of subjects, a dimensionality reduction technique, such as principal component analysis (PCA), was applied before the classifier [4,24].

This study was performed on baseline MRI data from the ADNI study. All subjects underwent clinical/cognitive assessment at the time of scan acquisition. As part of each subject's cognitive evaluation, the Mini-Mental State Examination (MMSE) was performed to provide a global measure of mental status [8]. The Clinical Dementia Rating (CDR) was also assessed as a measure of dementia severity [13]. The elderly normal subjects had no symptoms of depression, mild cognitive impairment, or other forms of dementia. All AD subjects met NINCDS/ADRDA criteria for probable AD [18].

All exclusion and inclusion criteria from the ADNI protocol were applied to the selected AD and NOR subjects [19]; refer to the ADNI protocol for detailed inclusion and exclusion criteria. Finally, 172 AD subjects (87 males, 85 females, $age \pm standard\ deviation = 75 \pm 8$ years, range = 55–91 years, MMSE=23.2 ± 2.1, range = 18–27, CDR = 1.0 ± 0.3, range = 0.5–2) and 186 normal control subjects (NOR) (94 males, 92 females, age = 76 ± 5 years, range = 60–90 years, MMSE = 29 ± 1, range = 25–30, CDR = 0 for all NOR subjects) were considered for this study. Two independent datasets were defined using random allocation: 240 subjects for training (120 AD, 120 NOR) and 100 subjects for testing (50 AD and 50 NOR), both gender-matched. The random allocation was executed 20 times, yielding 20 different pairs of training–testing datasets. Note that in each random allocation 18 subjects were not assigned to any group, in order to assure gender-matched groups in both trainig and testing dataset. For each allocation the training dataset was used to estimate the statistical masks.

High-resolution structural brain MRI scans were acquired at ADNI sites with 1.5 T MRI scanners using the standard ADNI MRI protocol. For each subject, two T1 MRI scans were collected using a sagittal 3D MP-RAGE sequence with voxel size of $0.94\,mm \times 0.94\,mm \times 1.2\,mm$. The images were calibrated with phantom-based geometric corrections to ensure consistency among scans acquired at different sites. Additional image corrections included geometric distortion correction, bias field correction and geometrical scaling. See [19] for more details. The preprocessed images are available to the scientific community and were downloaded from the ADNI website.

In this study the anatomical feature was the local volume change of the mapping between an unbiased atlas and each subject [2]. The unbiased atlas was estimated once from 40 normal elderly subjects. Although these 40 subjects take part in the dataset for random allocation, it has been forced that neither of these 40 subjects ever fall within any testing dataset. The resolution of the atlas was isotropic. Non-rigid registration was performed using a stationary velocity field diffeomorphic registration, that provided high resolution Jacobian fields [2]. The Jacobian determinant of the spatial transformation is the atrophy/expansion factor at each voxel in atlas coordinates. As these scalar values are positive, they are intrinsically skew-distributed, and the logarithm transformation was applied to make its distribution more symmetric. The Jacobian determinant fields were masked with either statistical or anatomical masks.

The *statistical masks* for each allocation were defined by the voxels with the largest significant difference in a group comparison statistical map performed on the corresponding training dataset. Voxel-wise Student's *t*-test was performed on the log of Jacobian determinants in the whole brain. As shown in [2], the statistical maps between subject groups obtained by using stationary velocity field diffeomorphic registration provided better spatial resolution and larger significance when compared with previous works [12]. Three threshold values, $th_t = 6$, 8 and 10, were applied to the absolute value of Student's *t* statistic, providing larger, medium and smaller masks respectively with different significance. If the sign of the t statistic is considered, negative values correspond with volume expansion while positive values correspond with atrophy. Fig. 1 shows the boundary of the masks corresponding to the average of the *t*-test maps. The number of voxels of these average masks was 10399, 3065 and 948 corresponding to $th_t = 6$, 8 and 10.

The *anatomical masks* were obtained by using FIRST segmentation tool [20] from FSL package [23] on the atlas. Three regions were selected: both amygdalae (Amyg), hippocampi (Hipp), and lateral ventricles (Late). Segmentation of the lateral ventricles was manually edited to include the temporal horns. The number of voxels of each mask was 4448, 8272 and 41540 respectively. Two additional masks were generated as the union of the three previous masks (Amyg–Hipp–Late), and the union of the amygdalae and hippocampi (Amyg–Hipp) masks.

These two types of masks provided an important dimensionality reduction while preserving relevant features. However the number of selected features was still larger than the number of subjects and PCA was used to reduce further the dimensionality.

For the purposes of this study we selected five standard classifiers, namely Linear and Quadratic Discriminant Analysis (LDA, QDA) and Support Vector Machine (SVM) classifiers using three different kernels: linear kernel with a Least Squares (LS) optimization technique and a constraint size on the margin of 10^6 (svmL-LS6); quadratic (svmQ-QP) and cubic polynomial kernels (svmP-QP) with a quadratic programming (QP) optimization technique. Classification experiments were computed using MATLAB (The MathWorks, Natick, MA). Classification performance was assessed on the 20 pairs of training–testing datasets. Performance was measured in terms of classification accuracy.

Two discrimination models were analyzed. Model I used only atrophy/expansion features considering the first *n* PCA coefficients. Model II was an extension of Model I by adding demographic information (age and gender) and ApoE allele genotype for each subject. The combination of three different ApoE alleles ($\epsilon 2$, $\epsilon 3$, and $\epsilon 4$) give six possible genotypes. FeaApoE is an integer that represents such combinations: $1 = (\epsilon 2, \epsilon 2)$; $2 = (\epsilon 2, \epsilon 3)$; $3 = (\epsilon 2, \epsilon 4)$; $4 = (\epsilon 3, \epsilon 3)$; $5 = (\epsilon 3, \epsilon 4)$; and $6 = (\epsilon 4, \epsilon 4)$. The input features to Model II was {Age; Sex; FeaApoE; first PCA coefficients}.

The classification accuracy for Model II outperformed Model I when using either statistical or anatomical masks and for all classifiers except for the svmP–QP classifier. The difference ranged from 0% to 12%, with a maximum accuracy of 95%. For brevity reasons and to facilitate comparison with previous studies only Model I performance is shown in Fig. 2. The best performance among the anatomical masks (upper panel in Fig. 2) was obtained by the union of both amygdalae and hippocampi (Amyg–Hipp) considering a compromise between the following criteria in the Model I and II:

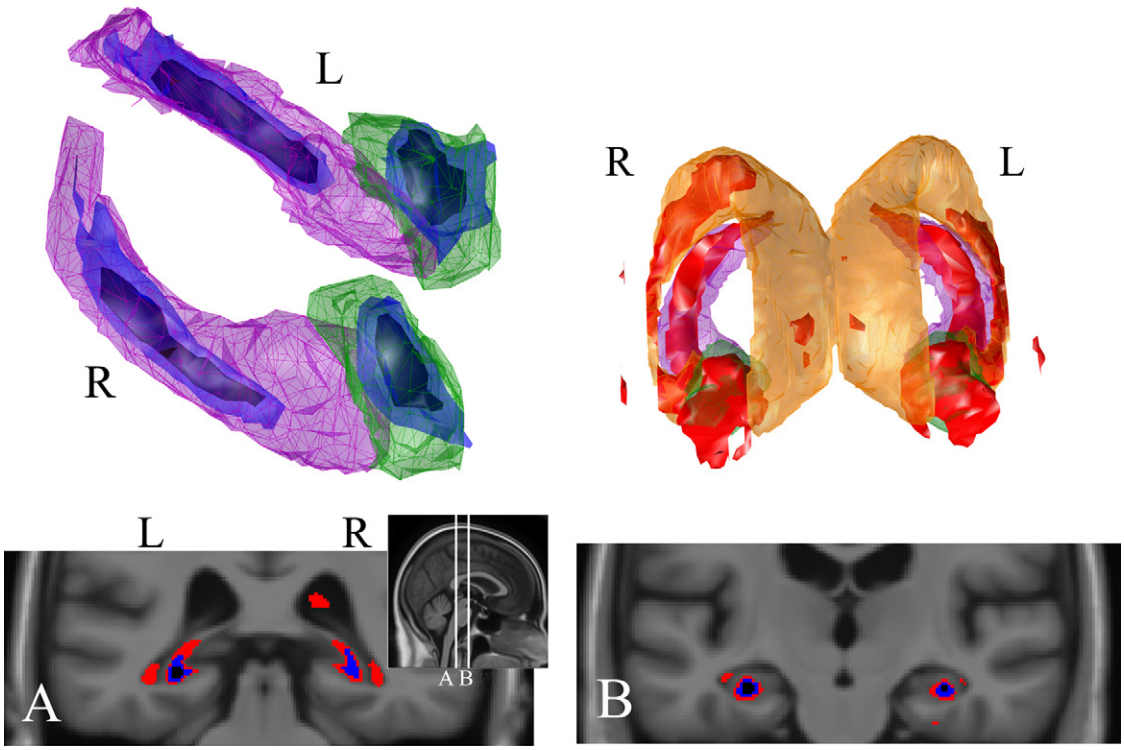

Fig. 1. Illustration of the statistical masks defined by threshold values $th_t = 10$ in black, $th_t = 8$ in blue, and $th_t = 6$ in red, obtained from the average t-test map. Top: Surface representations of the anatomical and statistical masks (amygdalae in green, hippocampi in purple and lateral ventricles in orange). The top right panel is a video in the electronic version: The last video sequence shows the mask $th_t = 6$ with two colors, atrophy in red and expansion in turquoise. Bottom: Two coronal MRI slices of the atlas with the statistical masks overlaid with the same color criteria.

better performance in the worst case (0.25th percentile), better performance in an average case (represented as the median score) as well as better performance in the best case (99.75th percentile). Regarding to the statistical masks (bottom panel in Fig. 2, the mask defined by the threshold value $th_t = 8$ obtained the best accuracy performance following the same criteria as before.

Fig. 2 shows that the performance of the classifiers degrades when using large enough number of PCA coefficients, being this decline more pronounced in the more complex classifiers.

In order to compare the performance between the best statistical mask ($th_t = 8$) and the best anatomical mask (Amyg–Hipp), the accuracy difference was computed for each of the 20 random allocations. The anatomical mask ($th_t = 8$) outperformed the Amyg–Hipp mask in 83% of the 20 experiments when using from 1 to 4 PCA coefficients. The median difference was of 5% for the first PCA coefficient, which was the coefficient where more differences between the two masks were found.

The main interest of the present work was to find the most relevant brain strucutures/regions for NOR–AD discrimination using brain atrophy/expansion features computed from MR images. To this end five classifiers with different complexity levels were used. According to the results in Fig. 2, the use of more complex classifiers did not generally provide a better performance.

As mentioned in Introduction, three major design criteria for the classification algorithm were used: small number of features, generalizability, and amenability to anatomical interpretation of the selected features.

As regards generalizability, classification performance was assessed in this work using 20 experiments where subjects were randomly allocated to either training or testing datasets. In contrast, previous works used either leave-one-out experiments, providing an optimistic score, [9,4] or single training-test experiments [26]. Interestingly, the variability of the performance found among the 20 experiments was higher than the performance difference obtained using different classifiers. Accordingly, several random allocations of subjects should be used for a reliable assessment of the perfomance.

The second criterion was imposed because the number of raw features in medical imaging studies is very high. Therefore, feature reduction is required in order to keep a feature set dimension small enough as compared to the population size. In previous works: 237 features were selected from a training set of 280 subjects and yielded an 89% classification accuracy on an independent testing set of 100 subjects [26]; using 16 features with a SVM classifier a classification accuracy of 94% was obtained on a population of 48 subjects [9]; about 84% accuracy was found using either a median of 7 features with an LDA classifier or a median of 12 features with a QDA where the size of the validation set was 150 subjects [4]. In contrast, in this work a median classification accuracy of 82% (maximum of 91%, minimum of 78%), in Model I, was achieved even for a simple QDA classifier with only 3 features for the statistical mask $th_t = 10$, on 20 different subsamplings of 240 training subjects and 100 test subjects. That is, similar results were obtained in this work, but using a smaller number of features and a more demanding validation; hence, the proposed algorithm has been shown to be more robust and simple.

Regarding the anatomical interpretation, some previous studies did not offer a detailed interpretation of the relevant features [4,9], except for Vemuri et al. [26]. The main feature extraction technique used in this work, either an anatomical or a statistical mask, allows a anatomical interpretation. The masks with the best classification performance identify the brain regions with relevant volume changes for NOR–AD discrimination. The statistical masks $th_t = 8$ and 10 were found in voxels belonging to the hippocampi and amygdalae (see video in Fig. 1). This is concordant with the well-known fact that both hippocampi and amygdalae are structures that suffer atrophy from the earlier stages of AD

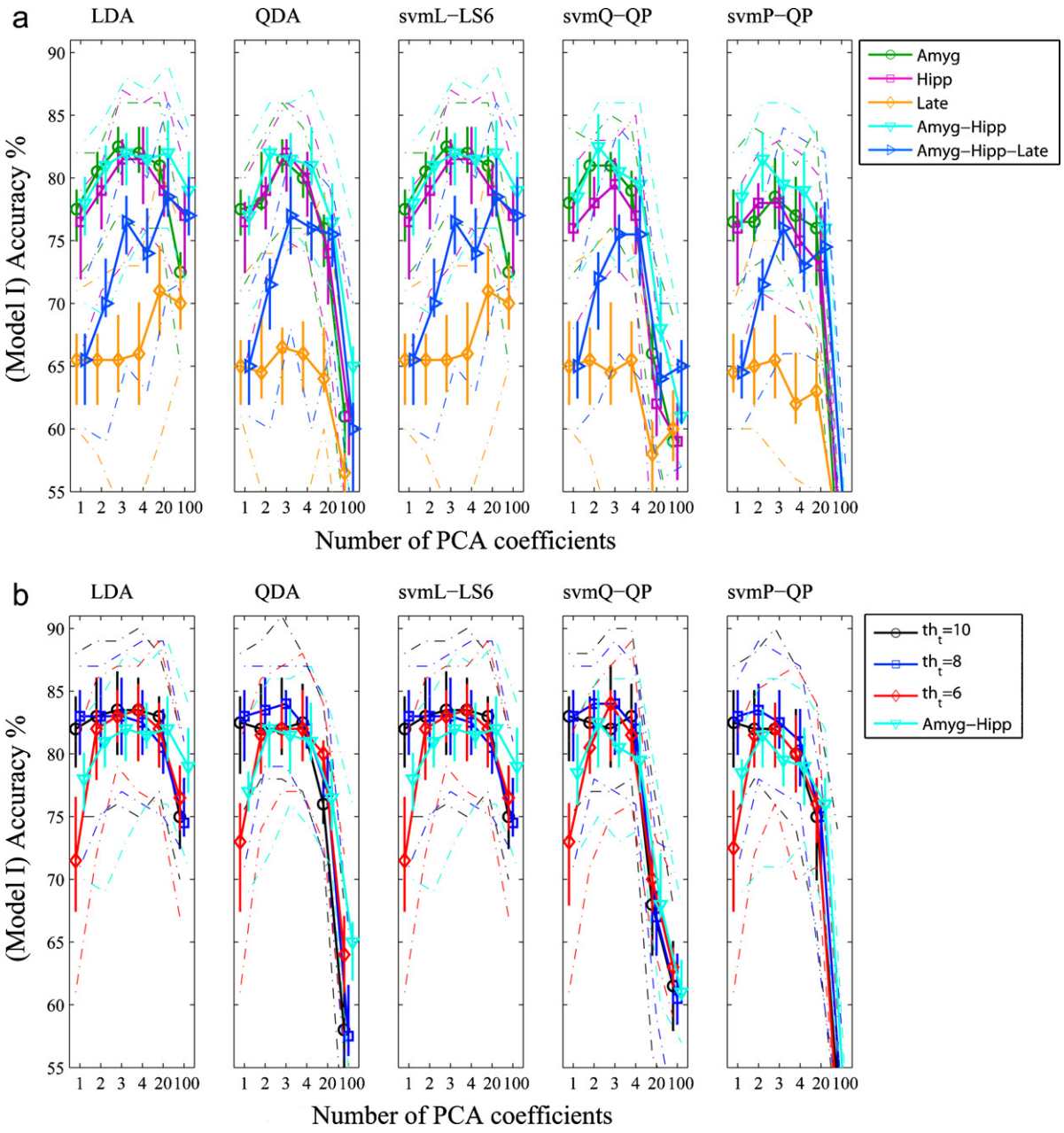

Fig. 2. Illustration of classification accuracy of Model I for the 20 random allocations, the five selected classifiers with different number of features. Upper panel: anatomical masks. Bottom panel: statistical masks. For each working condition (classifier type and number of features) accuracy results are represented as follows: median score as markers, interquartile range as vertical bars, and the (99.75, 0.25)-th percentile as dashed lines.

[3]. Three hippocampus substructures, subiculum, CA1 regions and dentate gyrus-hilar region, account for the majority of the voxels within statiscal masks $th_t = 8$, 10. This result is in agreement with other statistical studies (see [21] and references therein). As for the statistical mask $th_t = 6$, it reached a performance accuracy similar to the other statistical masks for a larger number of PCA coefficients. This larger statistical mask significant atrophy extends to the isthmus of cingulate gyrus and the crus of fornix, which are close and connected to the hippocampus, and significant volume increase of the temporal horns of the ventricles (see video and panel in Fig. 1). The relationship between the lateral horns and AD has been reported by other studies [6,25]. Furthermore, the lateral ventricle expansion may be also caused by normal aging, while the amygdala and the hippocampi, structures being close to the lateral horns, have been reported to exhibit small or no age effect [10].

The contributions of this work relative to previous studies are: first, an extensive validation with 20 different subsamplings of subjects, which highlights the variability existing in the results of classification caused by this subsampling; second, an anatomical interpretation of the used masks corroborated by the results in the classification; third, non-rigid registration was performed using a stationary velocity field diffeomorphic registration, that provide high resolution Jacobian fields.

And finally in this work, the classification performance obtained using the statistical mask $th_t = 8$ exceded in most cases the ones obtained with the anatomical masks. Another advantage of the statistical masks was that they allowed to highlight the heterogeneity of anatomical regions, identifying which areas of these regions or subfields are best suited for classifying subjects with AD. All in all, it has been shown that statistical masks provide better performance than anatomical masks under the conditions of this study.

Acknowledgements

This work was partially funded by research grants TEC2009-14587-C03-01 from CICYT, TSI-020110-2009-362 from MITC and PI100/08 from Diputacion General Aragon, Spain.

Data collection and sharing for this project was funded by the Alzheimer's Disease Neuroimaging Initiative (ADNI; Principal Investigator: MichaelWeiner; NIH grant U01 AG024904). This research was also supported by NIH grants P30 AG010129, K01 AG030514, and the Dana Foundation.

Appendix A. Supplementary data

Supplementary data associated with this article can be found, in the online version, at doi:10.1016/j.neulet.2010.10.007.

References

[1] H. Bickeboller, D. Campion, A. Brice, P. Amouyel, D. Hannequin, O. Didierjean, C. Penet, C. Martin, J. Pérez-Tur, A. Michon, B. Dubois, F. Ledoze, C. Thomas-Anterion, F. Pasquier, M. Puel, J. Demonet, O. Moreaud, M. Babron, D. Meulien, D. Guez, M. Chartier-Harlin, T. Frebourg, Y. Agid, M. Martinez, F. Clerget-Darpoux, Apolipoprotein E and Alzheimer disease: genotype-specific risks by age and sex, American Journal of Human Genetics 60 (2) (1997) 439–446.

[2] M. Bossa, E. Zacur, S. Olmos, Tensor-based morphometry with stationary velocity field diffeomorphic registration: application to ADNI, NeuroImage 51 (3) (2010) 956–969.

[3] H. Braak, E. Braak, Staging of Alzheimer's disease-related neurofibrillary changes, Neurobiology of Aging 16 (3) (1995) 271–278.

[4] S. Duchesne, A. Caroli, C. Geroldi, C. Barillot, G. Frisoni, D. Collins, MRI-based automated computer classification of probable AD versus normal controls, IEEE Transactions on Medical Imaging 27 (4) (2008) 509–520.

[5] D.A. Evans, H.H. Funkenstein, M.S. Albert, P.A. Scherr, N.R. Cook, M.J. Chown, L.E. Hebert, C.H. Hennekens, J.O. Taylor, Prevalence of Alzheimer's disease in a community population of older persons: higher than previously reported, JAMA 262 (18) (1989) 2551–2556.

[6] L. Ferrarini, W.M. Palm, H. Olofsen, M.A. van Buchem, J.H. Reiber, F. Admiraal-Behloul, Shape differences of the brain ventricles in Alzheimer's disease, NeuroImage 32 (3) (2006) 1060–1069.

[7] C.P. Ferri, M. Prince, C. Brayne, H. Brodaty, L. Fratiglioni, M. Ganguli, K. Hall, K. Hasegawa, H. Hendrie, Y. Huang, A. Jorm, C. Mathers, P.R. Menezes, E. Rimmer, M. Scazufca, Global prevalence of dementia: a Delphi consensus study, The Lancet 366 (9503) (2006) 2112–2117.

[8] M. Folstein, S. Folstein, P. McHugh, Mini-mental state. A practical method for grading the cognitive state of patients for the clinician, Journal of Psychiatric Research 12 (1975) 189198.

[9] E. Gerardin, G. Chételat, M. Chupin, R. Cuingnet, B. Desgranges, H.-S. Kim, M. Niethammer, B. Dubois, S. Lehéricy, L. Garnero, F. Eustache, O. Colliot, Multidimensional classification of hippocampal shape features discriminates Alzheimer's disease and mild cognitive impairment from normal aging, NeuroImage 47 (4) (2009) 1476–1486.

[10] C.D. Good, I.S. Johnsrude, J. Ashburner, R.N.A. Henson, K.J. Friston, R.S.J. Frackowiak, A voxel-based morphometric study of ageing in 465 normal adult human brains, NeuroImage 14 (1) (2001) 21–36.

[11] M. Grundman, D. Sencakova, C. Jack Jr., R. Petersen, H. Kim, A. Schultz, M. Weiner, C. DeCarli, S. DeKosky, C. van Dyck, R. Thomas, L. Thal, Brain MRI hippocampal volume and prediction of clinical status in a mild cognitive impairment trial, Journal of Molecular Neuroscience 19 (2002) 23–27.

[12] X. Hua, A.D. Leow, S. Lee, A.D. Klunder, A.W. Toga, N. Lepore, Y.-Y. Chou, C. Brun, M.-C. Chiang, M. Barysheva, C.R. Jack Jr., M.A. Bernstein, P.J. Britson, C.P. Ward, J.L. Whitwell, B. Borowski, A.S. Fleisher, N.C. Fox, R.G. Boyes, J. Barnes, D. Harvey, J. Kornak, N. Schuff, L. Boreta, G.E. Alexander, M.W. Weiner, P.M. Thompson, I. The Alzheimer's Disease Neuroimaging, 3D characterization of brain atrophy in Alzheimer's disease and mild cognitive impairment using tensor-based morphometry, NeuroImage 41 (1) (2008) 19–34.

[13] C. Hughes, L. Berg, W. Danziger, L. Coben, R. Martin, A new clinical scale for the staging of dementia, The British Journal of Psychiatry 140 (1982) 566–572.

[14] C. Jack Jr., D. Dickson, J. Parisi, Y. Xu, R. Cha, P. O'Brien, S. Edland, G. Smith, B. Boeve, E. Tangalos, E. Kokmen, R. Petersen, Antemortem MRI findings correlate with hippocampal neuropathology in typical aging and dementia, Neurology 58 (2002) 750–757.

[15] C. Jack Jr., M. Slomkowski, S. Gracon, T. Hoover, J. Felmlee, K. Stewart, Y. Xu, M. Shiung, P. O'Brien, R. Cha, D. Knopman, R. Petersen, MRI as a biomarker of disease progression in a therapeutic trial ofmilameline for AD, Neurology 60 (2003) 253–260.

[16] H. Lemaître, F. Crivello, B. Grassiot, A. Alpérovitch, C. Tzourio, B. Mazoyer, Age- and sex-related effects on the neuroanatomy of healthy elderly, NeuroImage 26 (3) (2005) 900–911.

[17] A. Leow, A. Klunder, C. Jack Jr., A. Toga, A. Dale, M. Bernstein, P. Britson, J. Gunter, C. Ward, J. Whitwell, B. Borowski, A. Fleisher, N. Fox, D. Harvey, J. Kornak, N. Schuff, C. Studholme, G. Alexander, M. Weiner, P. Thompson, Longitudinal stability of MRI for mapping brain change using tensor based morphometry, NeuroImage 31 (2006) 627–640.

[18] G. McKhann, D. Drachman, M. Folstein, R. Katzman, D. Price, E.M. Stadlan, Clinical diagnosis of Alzheimer's disease: report of the NINCDS-ADRDA Work Group* under the auspices of Department of Health and Human Services Task Force on Alzheimer's Disease, Neurology 34 (7) (1984), 939–.

[19] S. Mueller, M. Weiner, L. Thal, R. Petersen, C. Jack, W. Jagust, J. Trojanowski, A. Toga, L. Beckett, Ways toward an early diagnosis in Alzheimer's disease: the Alzheimer's Disease Neuroimaging Initiative (ADNI), Alzheimer's & Dementia 1 (2005) 55–66.

[20] B. Patenaude, Bayesian Statistical Models of Shape and Appearance for Subcortical Brain Segmentation, Ph.D. thesis, 2007.

[21] A. Scher, Y. Xu, E. Korf, L. White, P. Scheltens, A. Toga, P. Thompson, S. Hartley, M. Witter, D. Valentino, L. Launer, Hippocampal shape analysis in Alzheimer's disease: a population-based study, NeuroImage 36 (1) (2007) 8–18.

[22] L. Silbert, J. Quinn, M. Moore, E. Corbridge, M. Ball, G. Murdoch, G. Sexton, J. Kaye, Changes in premorbid brain volume predict Alzheimer's disease pathology, Neurology 61 (2003) 487–492.

[23] S.M. Smith, M. Jenkinson, M.W. Woolrich, C.F. Beckmann, T.E.J. Behrens, H. Johansen-Berg, P.R. Bannister, M.D. Luca, I. Drobnjak, D.E. Flitney, R.K. Niazy, J. Saunders, J. Vickers, Y. Zhang, N.D. Stefano, J.M. Brady, P.M. Matthews, Advances in functional and structural MR image analysis and implementation as FSL, NeuroImage 23 (1) (2004) 208–219.

[24] C.E. Thomaz, F.L.S. Duran, G.F. Busatto, D.F. Gillies, D. Rueckert, Multivariate statistical differences of MRI samples of the human brain, Journal of Mathematical Imaging and Vision 29 (2–3) (2007) 95–106.

[25] P.M. Thompson, K.M. Hayashi, G.I. de Zubicaray, A.L. Janke, S.E. Rose, J. Semple, M.S. Hong, D.H. Herman, D. Gravano, D.M. Doddrell, A.W. Toga, Mapping hippocampal and ventricular change in Alzheimer disease, NeuroImage 22 (4) (2004) 1754–1766.

[26] P. Vemuri, J.L. Gunter, M.L. Senjem, J.L. Whitwell, K. Kantarci, D.S. Knopman, B.F. Boeve, R.C. Petersen, C.R. Jack Jr., Alzheimer's disease diagnosis in individual subjects using structural MR images: validation studies, NeuroImage 39 (3) (2008) 1186–1197.

[27] A. Wimo, B. Winblad, H. Aguero-Torres, E. von Strauss, The magnitude of dementia occurrence in the world, Alzheimer Disease & Associated Disorders 17 (2) (2003) 63–67.